Orbital occupation, atomic moments, and magnetic ordering at interfaces of manganite thin films

C. Aruta,[1,*] G. Ghiringhelli,[2] V. Bisogni,[3] L. Braicovich,[2] N. B. Brookes,[3] A. Tebano,[4] and G. Balestrino[4]
[1]*CNR-INFM Coherentia, Dipartimento di Scienze Fisiche, Università di Napoli "Federico II," Complesso di Monte S. Angelo, Via Cinthia, I-80126 Napoli, Italy*
[2]*CNR-INFM Coherentia and Soft, Dipartimento di Fisica, Politecnico di Milano, piazza Leonardo da Vinci 32, I-20133 Milano, Italy*
[3]*European Synchrotron Radiation Facility, Boîte Postale 220, F-38043 Grenoble, France*
[4]*CNR-INFM Coherentia and Dipartimento di Ingegneria Meccanica, Università di Roma Tor Vergata, Via del Politecnico 1, I-00133 Roma, Italy*
(Received 19 November 2008; revised manuscript received 5 May 2009; published 28 July 2009)

We have performed x-ray linear and circular magnetic dichroism experiments at the Mn $L_{2,3}$ edge of the $La_{0.7}Sr_{0.3}MnO_3$ ultrathin films. Our measurements show that the antiferromagnetic (AF) insulating phase is stabilized by the interfacial rearrangement of the Mn 3*d* orbitals, despite the relevant magnetostriction anisotropic effect on the double-exchange ferromagnetic (FM) metallic phase. As a consequence, the Mn atomic magnetic-moment orientation and how it reacts to strain differ in the FM and AF phases. In some cases a FM insulating (FMI) phase adds to the AF and FM. Its peculiar magnetic properties include in-plane magnetic anisotropy and partial release of the orbital moment quenching. Nevertheless the FMI phase appears little coupled to the other ones.

DOI: 10.1103/PhysRevB.80.014431 PACS number(s): 75.47.Lx, 78.70.Dm

I. INTRODUCTION

Interfaces obtained by assembling insulating, nonmagnetic perovskite oxides can show unexpected properties such as high conductivity and ferromagnetism.[1,2] Oxygen vacancies,[3] epitaxial strain,[4,5] the so-called "polarization catastrophe" from interface-generated dipoles[6] and electronic reconstruction at the interface[7,8] are all at play in perovskite oxides and their individual roles are still far from being understood. An important case is the interface of manganites thin films with other different oxides, providing tunnel junctions for a number of manganite-based devices, such as spin valve or spin injectors. In this context, several authors have investigated the properties of ultrathin manganite films on various substrates and it has been found at the double-exchange (DE) magnetotransport properties are strongly depressed below a critical thickness.[9] To explain such a behavior, nanoscale inhomogeneities with coexisting clusters of different stable phases have been extensively investigated but it is still uncertain if and how this acts on the suppression of the magnetotransport properties of ultrathin films.[10] Chemical composition, strain, and oxygen stoichiometry are considered the main parameters influencing the disorder-driven phase separation.[11] In thin films of $La_{0.7}Sr_{0.3}MnO_3$ (LSMO) the existence of intrinsic inhomogeneities has been explained in terms of structural macroscopic distortions induced by the strain with the substrate which favors preferential orbital occupation of the e_g Mn orbitals.[12,13] While in the case of LSMO films grown on $LaAlO_3$ substrate the suppression of the DE magnetotransport properties is a "bulk" effect caused by strong in-plane compressive epitaxial strain, in the case of the LSMO films grown on $SrTiO_3$ (weak tensile strain) and $NdGaO_3$ (almost unstrained) the same phenomenon is a pure "interface/surface" effect.[14] Broken symmetry at the interfaces to the substrate and to the vacuum drives the orbital reorganization in ultrathin LSMO films, thus favoring the occupation of the $e_g(3z^2-r^2)$ versus the $e_g(x^2-y^2)$ orbitals among the otherwise energy degenerate Mn 3*d* states at the Mn^{3+} sites, as shown in Fig. 1. In addition, it has been recently reported[15] that structure and stoichiometry gradually change at the interface of ultrathin LSMO films on $SrTiO_3(100)$ (STO), with a resulting elongation of the interfacial out-of-plane lattice constant. Such structural modification is similar to the cooperative Jahn-Teller-type distortion induced by the in-plane compressive strain, which in turn favors the stabilization of the $e_g(3z^2-r^2)$ orbitals. As a result, the disproportion in e_g orbital occupation induces a coupling between neighboring Mn cations, that is, ferromagnetic (FM) along the *c* axis (perpendicular to the surface) and antiferromagnetic (AF) in the *ab* plane,[16] eventually resulting in the stabilization of the *C*-type AF phase at low temperature.[17] However, such magnetic phase was not directly experimentally observed.

While the bulk magnetic properties have been largely investigated in manganite films as a function of the strain,[18–21] the microscopic origin of the magnetic properties at the films surface and at the interface between film and substrate have not yet been completely clarified. In this respect experimental investigations by surface sensitive x-ray magnetic scattering of layered manganite single crystals[22] and of perovskite manganite thin films[23] have shown that the average in-plane FM ordering of the surface is significantly suppressed over a length scale of about 4 unit cells (u.c.) from the surface, even at low temperature. However, those measurements alone cannot discriminate between a homogeneous suppression of the magnetization over the surface and the coexistence of FM and AF phases. Thus, to detect both AF and FM phases, we have chosen two magnetically complementary techniques such as x-ray magnetic linear dichroism (XMLD) and x-ray magnetic circular dichroism (XMCD) in soft x-ray absorption spectroscopy (XAS) by synchrotron radiation. Such techniques were already successfully employed to observe the directional coupling by exchange bias between the spins in the AF regions and those in the adjacent FM regions in different magnetic systems.[24] Therefore, XMLD and XMCD

 ©2009 The American Physical Society

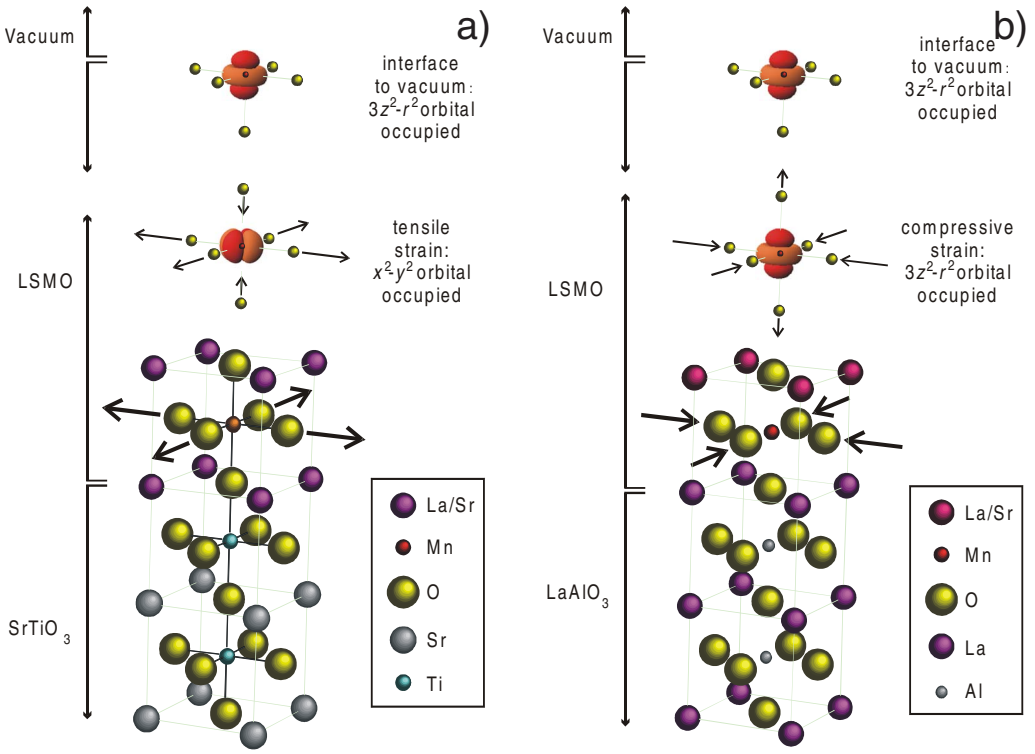

FIG. 1. (Color online) Schematics of the influence of strain onto the orbital occupation in the bulk and at the interface of LSMO films. The bulk Mn $3d$ orbital occupation is x^2-y^2 and $3z^2-r^2$ in case of (a) $SrTiO_3$ and (b) $LaAlO_3$ substrate, respectively. The preferential orbital occupation is $3z^2-r^2$ at both interfaces.

are the ideal techniques to study the arrangement of spins, together with the orbital occupancy, at interfaces in manganite films where AF and FM phases coexist on a nanometric scale. While strain-induced selective orbital occupancy has been recently reported in Refs. 25 and 26, the orbital reconstruction at the interface has been questioned by Huijben *et al.*,[27] on the basis of apparently very different linear dichroism (XLD) experimental results. Actually the XLD of Ref. 27 is not totally incompatible with that of Ref. 14 if one takes into account the fact that the former were measured at low temperature, where the magnetic contribution to XLD is strong, whereas the latter were taken above the Curie temperature, where the only contribution to XLD comes from the preferential orbital occupation. Moreover the interpretation given by Huijben *et al.*[27] of the XLD is surprisingly opposite to that of numerous papers with experimental and theoretical contents.[12,13,28] Interestingly, Huijben *et al.*[27] have also reported that the spin-to-orbital-ordered coupled insulator phase develop at the interface. Therefore, the microscopic origin of the magnetotransport properties at the interface of LSMO films is still under debate. Here we report the experimental evidence of the spin-orbit-lattice coupling at the interface of LSMO films. To achieve this result, we have compared LSMO films grown on STO, $NdGaO_3$(110) (NGO), or $LaAlO_3$(100) (LAO), and having different thicknesses so to have different strain conditions and to cross the metal-insulator transition at different temperatures. The high surface sensitivity of both XMLD and XMCD allowed to obtain information on the very thin LSMO layer at the interface with the substrate.

II. EXPERIMENT

LSMO films were grown by pulsed laser deposition with *in situ* reflection high-energy electron diffraction (RHEED). Film thickness was controlled at the level of a single unit cell by the intensity oscillations of the RHEED specular spot. Additional details on the growth technique are given in Ref. 29. The crystallographic and transport properties of the investigated samples, obtained by x-ray diffraction and electrical measurements,[12–14] are reported in Table I. The out-of-plane (ϵ_{zz}) and in-plane (ϵ_{xx}) strains are defined as the percentage variation in the out-of-plane and in-plane lattice parameters of films relative to the bulk LSMO values. From Table I it can be noticed that, in the case of the LAO substrate, the 30-u.c.-thick film is fully strained (in-plane compressive) while strain is partially relaxed in the 100-u.c.-

TABLE I. Out-of-plane (ϵ_{zz}) and in-plane (ϵ_{xx}) strain values and metal-insulator transition temperatures (T_{MI}) for LSMO films grown on the different substrates with different thickness. The samples are listed by decreasing transition temperature.

Substrate	Thickness (u.c.)	T_{MI} (K)	ϵ_{zz} (%)	ϵ_{xx} (%)
LAO	100	360	1.30	−1.70
STO	50	360	−1.10	0.90
STO	10	275	−1.10	0.90
NGO	9	200	0.20	−0.20
LAO	30		3.60	−2.20

thick film. Films on STO substrates are fully strained (in-plane tensile) regardless of film thickness. Finally, because of the good lattice match with the substrate, thin films on NGO result to have lattice parameters only slightly distorted relative to the bulk. The metal-insulator transition temperatures (T_{MI}) reported in Table I demonstrate that the suppression of the magnetotransport properties is strain dependent in case of LAO but is an interface effect in case of STO and NGO.[14]

Linear and circular dichroism measurements were carried out at the ID08 beam line of the European Synchrotron Radiation Facility by tuning the synchrotron radiation at the Mn L edge. The dominant photon-excited transitions are $2p \rightarrow 3d$, as detected by total electron yield. Spin-orbit interaction splits the L-edge absorption spectra into the L_3 and L_2 edges with opposite spin-orbit coupling ($l+s$ and $l-s$, respectively). A reversible and tunable (up to 1 T) external magnetic field can be used to modify the dichroic response of the sample.

Circular dichroism is the difference in the absorption of photons with right-handed or left-handed circular polarization and linear dichroism (XLD) is the difference in the XAS measurement when the electric vector of the incident photons is rotated by 90°, by using synchrotron radiation with horizontal (H) and vertical (V) polarizations. In all the XAS measurements a constant background was fitted to the pre-edge region of the L_3 edge and subtracted from the spectra, which are then normalized to the edge jump set to unity above the L_2 edge.

The case of circular dichroism is simpler: the signal is proportional to the projection along the photon propagation direction of the sample magnetization vector, and, at the Mn $L_{2,3}$ edge, the effect is very strong [Fig. 2(a)]. Thanks, also, to its exceptional sensitivity (it can probe FM samples down to a fraction of monolayer thick), XMCD can be used as an element-specific magnetometric technique, as shown by the hysteresis loops in Fig. 2(b), obtained by the maximum peak intensity of the XMCD (about 642 eV) as a function of the applied magnetic field. In principle, orbital and spin magnetic moments can be obtained from the analysis of the XMCD spectra.

On the other hand, it has been shown theoretically and experimentally[30,31] that XLD can have two different contributions, either magnetic or related to the orbital occupation. If the direction of the spin system has a component in the plane perpendicular to the propagation direction of the x-ray beam it is possible, by changing the linear polarization from H to V, to observe a magnetic dichroic signal (XMLD), which can be nonzero also in the case of AF ordering.[32] Furthermore, if the Mn $3d$ orbitals are anisotropically populated, in addition to the magnetic contribution, an orbital contribution shows up in the XLD spectra.

III. RESULTS

The orbital contribution to XLD in Mn^{3+} is caused by the anisotropy in the bonding and is strictly related to the occupation of the $e_g(3z^2-r^2)$ or $e_g(x^2-y^2)$ orbitals. Because the magnetic order vanishes above the magnetic order temperature, XLD measurements performed at room temperature can

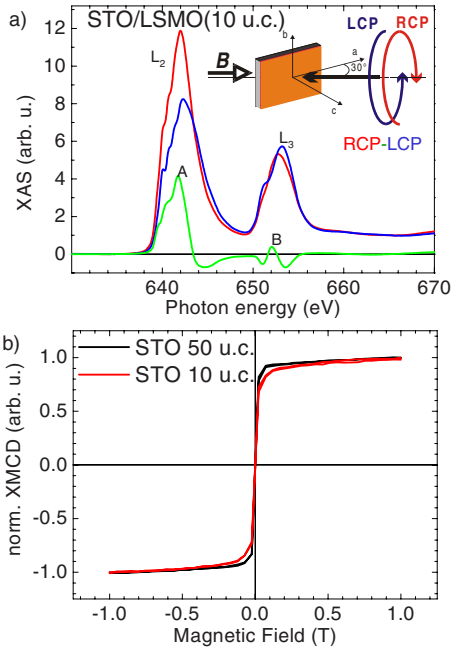

FIG. 2. (Color online) (a) Typical XAS and XMCD results for 10-u.c.-thick film on STO with an applied magnetic field of $B=1$ T. In the inset the experimental configuration is shown. The XMCD results are reported as a difference of the XAS measurements with right-circularly polarized (RCP) and left-circularly polarized (LCP) polarizations and without any further normalization. (b) Hysteresis loops curves between $B=-1$ T and $B=1$ T, for 50-u.c.-thick film and 10-u.c.-thick film on STO. The curves are normalized to unity for a better comparison of the coercive fields. All measurements in (a) and (b) were performed at temperature of $T=10$ K.

be only sensitive to the preferential orbital occupation. Room temperature XLD curves of Figs. 4(b) and 5(b) are typical of the $e_g(3z^2-r^2)$ preferential occupation induced by the interface symmetry in very thin films,[14] whatever the sign of the mismatch between film and substrate. Furthermore, below the magnetic transition temperature, by applying a magnetic field parallel to the incident photon beam, it is possible to suppress selectively the FM contribution to the XMLD spectrum thus singling out the AF contribution. In such a geometry, if the applied field is strong enough, magnetization in the FM system is forced to align along the direction of the incident beam. Therefore, the FM contribution to the XMLD is suppressed because the spin system is orthogonal to both the V and H polarization directions. On the other hand, spin orientation in the AF phase is not affected by an external field, so that no major changes in the XMLD spectra under external field are expected for the AF phase.

Normalized XLD spectra as a function of temperature for LSMO films grown on STO and LAO are reported in Figs. 4(b) and 5(b), taken with or without the applied magnetic field $B=1$ T. Such a field is strong enough to saturate the magnetization of the FM phase, as demonstrated by the hysteresis loops reported in Figs. 2(b) and 3(b). The normalized XLD spectra for a 10-u.c.-thick LSMO film on STO is shown in Fig. 4(b), with (bottom panel) or without (top panel) applied magnetic field. As reported in Table I, the

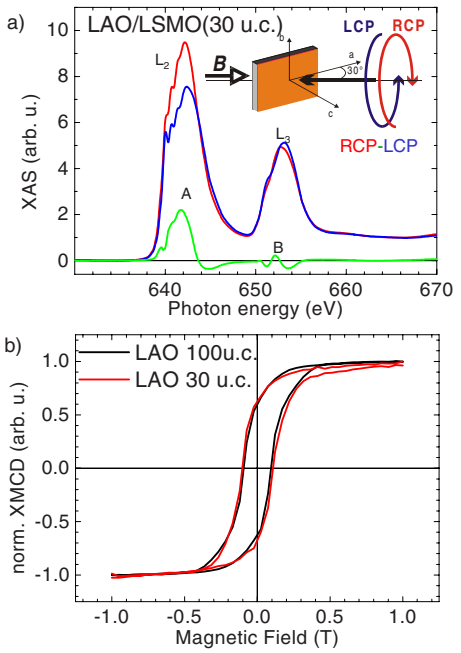

FIG. 3. (Color online) (a) Typical XAS and XMCD results for 30-u.c.-thick film on LAO with an applied magnetic field of $B=1$ T. In the inset the experimental configuration is shown. The XMCD results are reported as a difference of the XAS measurements with RCP and LCP polarizations and without any further normalization. (b) Hysteresis loops curves between $B=-1$ T and $B=1$ T, for 100-u.c.-thick film and 30-u.c.-thick film on LAO. The curves are normalized to unity for a better comparison of the coercive fields. All measurements in (a) and (b) were performed at temperature of $T=10$ K.

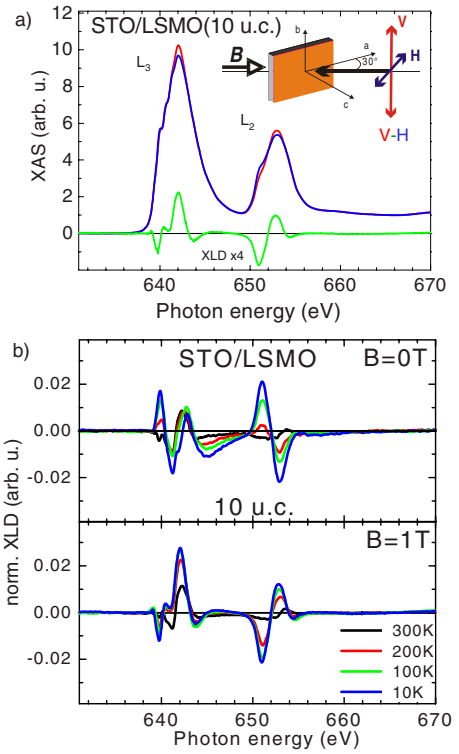

FIG. 4. (Color online) (a) Typical XAS and XLD (four times) results of 10-u.c.-thick LSMO film grown on STO substrate at temperature 10 K with the experimental configuration shown in the inset. XLD spectra are reported as the difference of the XAS measurements with V and H polarizations, without any further normalization. (b) Normalized XLD measurements without (top panels) and with (bottom panels) an external magnetic field $B=1$ T and at different temperatures ranging from 300 to 10 K. The spectra are normalized to the sum of the XAS L_3 peak height signals.

10-u.c.-thick film on STO has a depressed T_{MI} and becomes metallic only below 275 K because of the proximity to the critical thickness for the suppression of the magnetotransport properties (about 7 u.c. for films grown on STO and NGO).[14] XLD spectrum measured at 300K, above the magnetic transition temperature, is scarcely influenced by the application of a 1 T magnetic field, as expected. The intensity and shape of the XLD curves changes dramatically when the film is cooled below the magnetic ordering temperature. Large intensity changes in the XLD spectra with temperature reveal the magnetic dependence of the dichroic signal. Furthermore, below the ordering temperature, the application of a 1 T field along the x-ray beam direction results in a full reversal of the XLD curves relative to the zero-field case. Such an effect is a consequence of the field-induced suppression of the FM contribution to the XLD signal which is left with the AF contribution alone. The substantial presence of FM phase even in a sample with reduced T_{MI} is confirmed by the XMCD measurements of Figs. 2(a) and 2(b). The observed changing with temperature of the XLD shape is related to the different easy-axis orientation, i.e., local magnetic-moment preferential orientation, of the prevalent magnetic phase at the corresponding temperature.

A different behavior is shown in Fig. 5(b) for the 30-u.c.-thick film on LAO. In this case, the sizeable in-plane compressive epitaxial strain induced by the substrate strongly affects the magnetotransport properties,[13,14] thus resulting in an insulating behavior over the whole temperature range. The XLD spectra at $B=0$ T and $B=1$ T are similar at all temperatures indicating that the signal comes here mainly from an AF phase. Although, the XMCD measurements of Figs. 3(a) and 3(b) demonstrates the presence of a sizeable FM contribution even in this sample, in spite of the depressed magnetotransport properties. The domains dispersion of such FM metallic phase is supposed to be below the percolation limit for the charge transport because of the insulating character of the 30-u.c.-LSMO film on LAO. The additional presence at the interface of the Mn^{4+}-rich FM insulating (FMI) phase[13,33,34] has to be also considered.

In order to strengthen the scenario outlined above, we have subtracted the orbital contribution to the XLD spectra. To do this we assumed that the orbital contribution to XLD is negligibly sensitive to the temperature and plotted the difference between the XLD spectra measured below and above the magnetic ordering temperature: $I_{XMLD}=XLD_{10\ K}-XLD_{300\ K}$, where I_{XMLD} is the magnetic part of the linear dichroism signal. The I_{XMLD} spectra for LSMO samples with different thickness on STO and on LAO are shown in Fig. 6. XMLD spectra with $B=0$ T are sensitive to both the AF and FM phases while with $B=1$ T only the contribution of the AF phase is detected. 1 T is enough to saturate the FM phase in the given geometry as demonstrated by the hysteresis

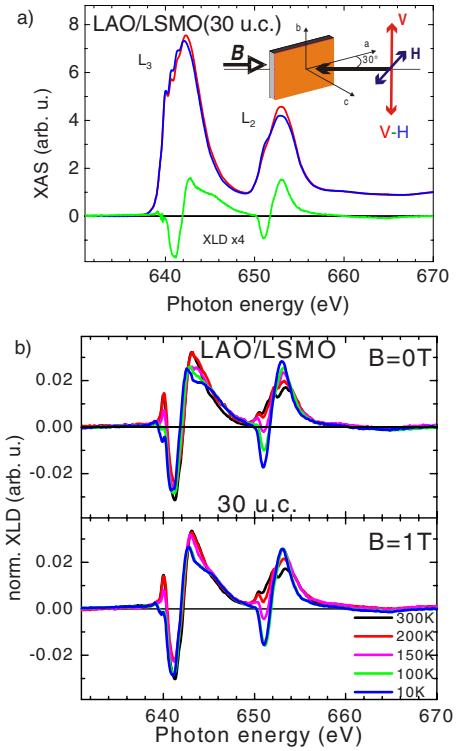

FIG. 5. (Color online) (a) Typical XAS and XLD (four times) results of 30-u.c.-thick LSMO film grown on LAO substrate at temperature 10 K with the experimental configuration shown in the inset. XLD spectra are reported as the difference of the XAS measurements with V and H polarizations, without any further normalization. (b) Normalized XLD measurements without (top panels) and with (bottom panels) an external magnetic field $B=1$ T and at different temperatures ranging from 300 to 10 K. The spectra are normalized to the sum of the XAS L_3 peak height signals.

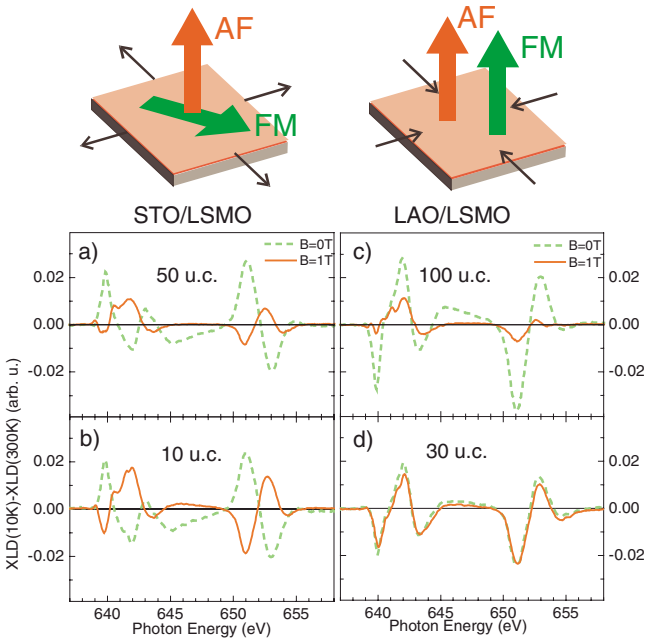

FIG. 6. (Color online) Difference between the XLD spectra taken at 10 and 300 K, with $B=0$ T and $B=1$ T, for the LSMO films: (a) 50 u.c. on STO, (b) 10 u.c. on STO, (c)100 u.c. on LAO, and (d) 30 u.c. on LAO (the same films of Fig. 3). All spectra are normalized to the sum of the XAS L_3 peak height signals. The schematics of the magnetization easy-axes directions are reported on the top of the figure for STO and LAO substrates on the left and on the right, respectively.

loops of Figs. 2(b) and 3(b). As reported in Table I, the 50-u.c.-thick film on STO [Fig. 6(a)] and the 100-u.c.-thick film on LAO [Fig. 6(c)] are both metallic above room temperature. The sizeable field-induced suppression of the difference spectrum in the case of the thicker film on LAO [Fig. 6(c)] indicates the predominance of the FM phase. On the contrary, when the film thickness is decreased [30 u.c. on LAO, Fig. 6(d)], the I_{XMLD} amplitudes at $B=0$ T and $B=1$ T become comparable, in agreement with the predominance of the AF phase. Moreover, it can be noticed that the FM and AF signals have the same qualitative behavior, which is a clear indication that the spin system has the same orientation in the two cases. On the other hand, it has been reported that the magnetization easy axis of manganite films grown under compressive strain (LAO substrates) is perpendicular to the substrate.[21] Therefore, both the FM and AF easy axes are perpendicular to the substrate (c axis). Such a finding, in agreement with the $e_g(3z^2-r^2)$ nature of the orbital contribution to XLD, confirms the development of the C-type AF phase, where spins are perpendicular to the substrate. For the two LSMO films on STO at $B=0$ T the curves are completely reversed with respect to those of films grown on LAO. This fact confirms that the easy magnetization axis of the FM phase is directed in the ab plane, as already reported in literature.[21] On the contrary, the difference spectra at $B=1$ T (when the FM phase is suppressed) have the same behavior as for the films on the LAO substrate (and on the NGO substrate too, not shown here). As a consequence, in LSMO films grown on STO and NGO the C-type AF phase is stabilized regardless of the small in-plane tensile strain, which would rather be expected to favor the A-type AF phase.[12,17,25,26] Therefore, in thin films grown on STO and NGO the FM easy axis lays in the ab plane whereas the AF easy axis is along the c axis. The schematic drawings of the different easy-axes directions are reported at the top of Fig. 6.

Further insight in the magnetic properties of very thin manganite layers can be obtained from XMCD measurements. The spin and orbital magnetic moments per atom, m_s and m_o, can, in principle, be quantified by applying the sum rules.[35–37] According to them, m_s and m_o are directly related to the dichroic difference intensities A and B [Figs. 2(a) and 3(a)], which are the L_3 and L_2 areas, respectively, of the XMCD spectra,

$$m_s \sim \frac{A-2B}{C}$$

and

$$m_o \sim \frac{A+B}{C},$$

where C is the XAS energy integral over the $L_{2,3}$ edges. However, the quantitative analysis with the sum rules is

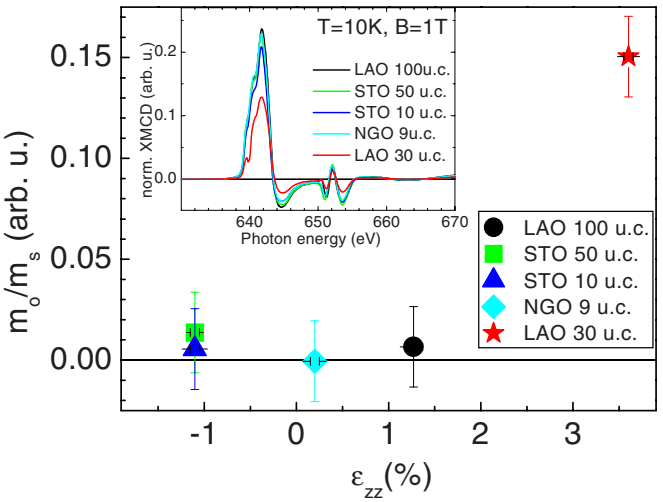

FIG. 7. (Color online) Orbital to spin moment ratio as a function of the out-of-plane strain for all investigated LSMO films on STO, NGO, and LAO substrates. The corresponding XMCD spectra, normalized to the sum of the XAS L_3 peak height signals, are reported in the inset.

demonstrated to fail in case of Mn atoms[38] because of the mixing of the L_3 and L_2 core levels and of the contribution of the magnetic dipole term. In Fig. 7 we report the ratio of the orbital to spin moment (m_o/m_s) as a function of the strain to qualitatively compare the investigated samples. It is also important to underline that the A and B values extracted from the XMCD data strongly depend on the energy range chosen for the integration of the L_3 and L_2 edges. Therefore, the determination of the orbital and spin moments is affected by a large uncertainty and can be carried out with the limited purpose of a comparison among homogenous measurements. In the inset of Fig. 7 the shape of the XMCD spectra is shown as a whole to highlight the different behaviors of the L_3 and L_2 edges. It follows that m_s decreases with the degradation of the magnetotransport properties, in agreement with a decrease in the FM phase content, while m_o is zero within our experimental error in all the samples except the 30-u.c.-thick film on LAO.

IV. DISCUSSION

Our XMLD and XMCD results can be explained in terms of the 3d orbital occupation and the coupling among lattice distortions and atomic moments. While XMCD technique was employed to detect the FM spin content, the complementary XMLD technique was used to investigate the anisotropy of the FM and AF phases.

By XMCD measurements, we observed a significant FM contribution also in the insulating 30-u.c.-thick LSMO film on LAO while such contribution was not detected by XMLD measurements. This finding can be an indication of the in-plane orientation of the FMI phase, thus being orthogonal to the out-of-plane-oriented FM metallic phase in LSMO films grown on LAO. Indeed, if the FMI and FM metallic phase are of similar amount they cancel out, as in the case of the 30-u.c.-thick film. On the contrary, in the 100 u.c. sample the FM metallic dominates and a large difference between the $B=0$ and $B=1$ T spectra can be observed in XMLD of Fig. 6. Using XMLD we found (see Fig. 6) that at the interfaces the AF C-type phase is nucleated by the stabilization of the $3z^2-r^2$ orbital due to the break of the symmetry along the c axis. This also leads to preferential spin orientation out of the ab plane in the AF phase, irrespective of the strain induced by the substrate. On the contrary in the FM regions we found a preferential orbital occupation within the ab plane for tensile strain (STO substrate) and out of the ab plane for compressive strain (LAO). As already reported in literature,[21] these results can be explained in terms of the positive magnetostriction which induces the FM easy axis along the tensile-strain direction. We can rule out the shape anisotropy contribution in agreement with previous reports[18] because in our films the FM easy-axis in-plane orientation is not strictly dependent on the thickness of the film. Because the DE FM phase is orbital disordered, the orbital occupation dependence of the interface anisotropy cannot play a role but it is only responsible for the spin direction in the orbital-ordered AF phase.

Moreover the evolution of m_o/m_s measured by XMCD reported in Fig. 7 demonstrates the lattice-distortion effect on the orbital moment. It can also be explained in the framework of coexisting clusters of AF and FM phases, plus a minority contribution from a FMI phase. In fact for cubic crystal field the orbital moment is expected, from elementary considerations, to be totally quenched.[39] That is, what happens when FM phase is predominant: the crystal-field tetragonal distortion is much smaller than the intrinsic width of the Mn states projected onto the O 2p band[12] and the orbital moment in the FM phase remains negligible despite local distortions arising from strain. When the thickness is reduced and the strain becomes more and more important the AF fraction increases and the total spin moment detected by XMCD decreases because XMCD is insensitive to AF moments. When the AF phase dominates (30 u.c. on LAO), a significant elongation of the octahedra along the z direction takes place also in the FM phase, the $e_g(3z^2-r^2)$ orbitals get preferentially occupied and the orbital moment quenching is partially lifted[18,40] because of the relevant contribution of the FMI phase. The nonquenched m_o value can also be explained in terms of the e_g occupancy decrease, as in the case of Mn^{4+} increasing of the interfacial FMI phase and the e_g-band-width narrowing.[40] The last being also related to the lattice distortions and the more ionic character of the FMI phase. All these effects might cooperatively contribute to deviate the orbital moment from the quenching in the thinnest LSMO film on LAO. Further investigation and theoretical calculations are required to better clarify the origin of the nonquenched orbital moment.

Finally we note that the AF and FM phases have rather independent magnetic anisotropy. From one side, the nonquenched in-plane m_o value is related to the FMI in-plane easy magnetic-axis orientation. On the other side, in the FM metallic phase the magnetization orientation is determined by the strain-induced magnetostriction. On the contrary, in the AF phase the preferential orbital occupation always leads to an out-of-plane spin orientation, irrespective of the strain conditions (Fig. 6). Therefore, in the phase separated state

the exchange bias between the AF and FM regions can be considered negligible and the spin alignment decoupled in the case of LSMO films on STO. However, we can guess that the FM/AF exchange-bias coupling is very small also in the case of LAO because the FMI phase is supposed to be in-plane oriented, thus orthogonal to both the metallic FM and the AF phases. In addition, despite the same spin orientation of the AF and the metallic FM phases in the films grown on LAO and the higher coercive fields, we have not observed any FM hysteresis loop shift by XMCD measurements, which is on the contrary expected in the case of a relevant FM/AF exchange-bias coupling.[41]

V. CONCLUSION

We have experimentally determined the microscopic origin of magnetic anisotropy in phase-separated LSMO thin films. The interfacial $e_g(3z^2-r^2)$ orbital occupation favors the *C*-type AF spin ordering. Thus, the easy axis of the AF phase is preferentially oriented perpendicularly to the *ab* plane for all the substrates, whatever the sign and the strength of the mismatch. On the contrary, in the FM phase the in-plane orbital magnetic moment is partially unquenched when the FMI content becomes relevant. In this case, the tetragonal distortion and the e_g-band-width narrowing relax the quenching of the orbital moment, giving rise to an effective spin-orbit coupling. This demonstrates that, in the magnetic coexisting phases, the spin-orbit to lattice coupling properties are different and magnetic anisotropy is quite independent.

ACKNOWLEDGMENTS

Fruitful discussions with V. Iannotti and A. Galdi are acknowledged.

*aruta@na.infn.it

[1] A. Brinkman, M. Huijben, M. Van Zalk, J. Huijbben, U. Zeitler, J. C. Maan, W. G. Van Der Wiel, G. Rijnders, D. H. A. Blank, and H. Hilgenkamp, Nature Mater. **6**, 493 (2007).
[2] A. Ohtomo and H. Y. Hwang, Nature (London) **427**, 423 (2004).
[3] A. Kalabukhov, R. Gunnarsson, J. Borjesson, E. Olsson, T. Claeson, and D. Winkler, Phys. Rev. B **75**,121404(R) (2007).
[4] H. Yamada, Y. Ogawa, Y. Ishii, H. Sato, M. Kawasaki, H. Akoh, and Y. Tokura, Science **305**, 646 (2004).
[5] K. H. Ahn, T. Lookman, and A. R. Bishop, Nature (London) **428**, 401 (2004).
[6] J. N. Eckstein, Nature Mater. **6**, 473 (2007).
[7] H. Zenia, G. A. Gehring, G. Banach, and W. M. Temmerman, Phys. Rev. B **71**, 024416 (2005).
[8] H. Zenia, G. A. Gehring, and W. M. Temmerman, New J. Phys. **9**, 105 (2007).
[9] J. Z. Sun, D. W. Abraham, R. A. Rao, and C. B. Eom, Appl. Phys. Lett. **74**, 3017 (1999); M. Bibes, S. Valencia, Ll. Balcells, B. Martínez, J. Fontcuberta, M. Wojcik, S. Nadolski, and E. Jedryka, Phys. Rev. B **66**, 134416 (2002); M. Angeloni, G. Balestrino, N. G. Boggio, P. G. Medaglia, P. Orgiani, and A. Tebano, J. Appl. Phys. **96**, 6387 (2004).
[10] J. Burgy, A. Moreo, and E. Dagotto, Phys. Rev. Lett. **92**, 097202 (2004); T. Becker, C. Streng, Y. Luo, V. Moshnyaga, B. Damaschke, N. Shannon, and K. Samwer, *ibid.* **89**, 237203 (2002); A. Biswas, M. Rajeswari, R. C. Srivastava, T. Venkatesan, R. L. Greene, Q. Lu, A. L. de Lozanne, and A. J. Millis, Phys. Rev. B **63**, 184424 (2001); Y. Murakami, J. H. Yoo, D. Shindo, T. Atou, and M. Kikuchi, Nature (London) **423**, 965 (2003).
[11] E. Dagotto, Science **309**, 257 (2005).
[12] C. Aruta, G. Ghiringhelli, A. Tebano, N. G. Boggio, N. B. Brookes, P. G. Medaglia, and G. Balestrino, Phys. Rev. B **73**, 235121 (2006).
[13] A. Tebano, C. Aruta, P. G. Medaglia, F. Tozzi, G. Balestrino, A. A. Sidorenko, G. Allodi, R. De Renzi, G. Ghiringhelli, C. Dallera, L. Braicovich, and N. B. Brookes, Phys. Rev. B **74**, 245116 (2006).
[14] A. Tebano, C. Aruta, S. Sanna, P. G. Medaglia, G. Balestrino, A. A. Sidorenko, R. De Renzi, G. Ghiringhelli, L. Braicovich, V. Bisogni, and N. B. Brookes, Phys. Rev. Lett. **100**, 137401 (2008).
[15] R. Herger, P. R. Willmott, C. M. Schlepütz, M. Björck, S. A. Pauli, D. Martoccia, B. D. Patterson, D. Kumah, R. Clarke, Y. Yacoby, and M. Döbeli, Phys. Rev. B **77**, 085401 (2008).
[16] J. B. Goodenough, Phys. Rev. **100**, 564 (1955).
[17] Y. Tokura and N. Nagaosa, Science **288**, 462 (2000).
[18] J. H. Song, J.-H. Park, J.-Y. Kim, B.-G. Park, Y. H. Jeong, H.-J. Noh, S.-J. Oh, H.-J. Lin, and C. T. Chen, Phys. Rev. B **72**, 060405(R) (2005).
[19] X. W. Wu, M. S. Rzchowski, H. S. Wang, and Q. Li, Phys. Rev. B **61**, 501 (2000).
[20] J. Dvorak, Y. U. Idzerda, S. B. Ogale, S. Shinde, T. Wu, T. Venkatesan, R. Godfrey, and R. Ramesh, J. Appl. Phys. **97**, 10C102 (2005).
[21] T. K. Nath, R. A. Rao, D. Lavric, C. B. Eom, L. Wu, and F. Tsui, Appl. Phys. Lett. **74**, 1615 (1999).
[22] J. W. Freeland, K. E. Gray, L. Ozyuzer, P. Berghuis, E. Badica, J. Kavich, H. Zheng, and J. F. Mitchell, Nature Mater. **4**, 62 (2005).
[23] J. J. Kavich, M. P. Warusawithana, J. W. Freeland, P. Ryan, X. Zhai, R. H. Kodama, and J. N. Eckstein, Phys. Rev. B **76**, 014410 (2007).
[24] F. Nolting, A. Scholl, J. Stöhr, J. W. Seo, J. Fompeyrine, H. Siegwart, J.-P. Locquet, S. Anders, J. Lüning, E. E. Fullerton, M. F. Toney, M. R. Scheinfeink, and H. A. Padmore, Nature (London) **405**, 767 (2000).
[25] L. Abad, V. Laukhin, S. Valencia, A. Gaup, W. Gudat, L. Balcells, and B. Martinez, Adv. Funct. Mater. **17**, 3918 (2007).
[26] I. C. Infante, F. Sanchez, J. Fontcuberta, M. Wojcik, E. Jedryka, S. Estrade, F. Peiro, J. Arbiol, V. Laukhin, and J. P. Espinos, Phys. Rev. B **76**, 224415 (2007).
[27] M. Huijben, L. W. Martin, Y.-H. Chu, M. B. Holcomb, P. Yu, G. Rijnders, D. H. A. Blank, and R. Ramesh, Phys. Rev. B **78**, 094413 (2008).

[28] D. J. Huang, W. B. Wu, G. Y. Guo, H.-J. Lin, T. Y. Hou, C. F. Chang, C. T. Chen, A. Fujimori, T. Kimura, H. B. Huang, A. Tanaka, and T. Jo Phys. Rev. Lett. **92**, 087202 (2004); H. B. Huang and T. Jo, Physica B **351**, 313 (2004); T. Jo, J. Electron Spectrosc. Relat. Phenom. **99**, 136 (2004).

[29] A. Tebano, G. Balestrino, N. G. Boggio, C. Aruta, B. Davidson, and P. G. Medaglia, Eur. Phys. J. B **51**, 337 (2006).

[30] M. W. Haverkort, S. I. Csiszar, Z. Hu, S. Altieri, A. Tanaka, H. H. Hsieh, H.-J. Lin, C. T. Chen, T. Hibma, and L. H. Tjeng, Phys. Rev. B **69**, 020408(R) (2004).

[31] G. van der Laan, E. Arenholz, R. V. Chopdekar, and S. P. Yuri, Phys. Rev. B **77**, 064407 (2008).

[32] P. Kuiper, B. G. Searle, P. Rudolf, L. H. Tjeng, and C. T. Chen, Phys. Rev. Lett. **70**, 1549 (1993); G. van der Laan, B. T. Thole, G. A. Sawatzky, J. B. Goedkoop, J. C. Fuggle, J. M. Esteva, R. Karnatak, J. P. Remeika, and H. A. Dabkowska, Phys. Rev. B **34**, 6529 (1986); J. Stöhr and S. Anders, IBM J. Res. Dev. **44**, 535 (2000).

[33] M. Bibes, Ll. Balcells, S. Valencia, J. Fontcuberta, M. Wojcik, E. Jedryka, and S. Nadolski, Phys. Rev. Lett. **87**, 067210 (2001).

[34] A. A. Sidorenko, G. Allodi, R. De Renzi, G. Balestrino, and M. Angeloni, Phys. Rev. B **73**, 054406 (2006).

[35] J. Stöhr and H. König, Phys. Rev. Lett. **75**, 3748 (1995).

[36] J. Stöhr, J. Electron Spectrosc. Relat. Phenom. **75**, 253 (1995).

[37] B. T. Thole, P. Carra, F. Sette, and G. van der Laan, Phys. Rev. Lett. **68**, 1943 (1992).

[38] K. W. Edmonds, N. R. S. Farley, T. K. Johal, G. van der Laan, R. P. Campion, B. L. Gallagher, and C. T. Foxon, Phys. Rev. B **71**, 064418 (2005).

[39] B. N. Figgis and M. A. Hitchman, *Ligand Field Theory and its Applications* (Wiley-VCH, New York, 2000), p. 241.

[40] T. Koide, H. Miyauchi, J. Okamoto, T. Shidara, T. Sekine, T. Saitoh, A. Fujimori, H. Fukutani, M. Takano, and Y. Takeda, Phys. Rev. Lett. **87**, 246404 (2001).

[41] J. Nogués and Ivan K. Schuller, J. Magn. Magn. Mater. **192**, 203 (1999).